13th World Conference on Earthquake Engineering
Vancouver, B.C., Canada
August 1-6, 2004
Paper No. 2722

PRECAST DIAPHRAGM PANEL JOINT CONNECTOR PERFORMANCE

Clay J. NAITO[1] and Liling CAO[2]

SUMMARY

To provide structural integrity to precast panel diaphragms, discrete web and chord connections are used. A wide variety of connection details are currently in use, however, a comprehensive evaluation has not been conducted. To address this issue an investigation of common connectors was made in consultation with US precast concrete producers and literature review. A detailed database of connectors in current use is presented and a comparison of their features is conducted. In addition a second database of connector performance is developed. This database includes all modeling features necessary for diaphragm modeling including stiffness, strength and deformation capacity. This information is used in conjunction with FEA to model a conventional floor diaphragm. Improved methods for accurately predicting the strength of connectors is proposed. In addition new simplified methods for directly estimating the diaphragm deformation is presented.

INTRODUCTION

Precast panels are commonly used for large floor systems in buildings and parking structures throughout the United States. Such systems are not only quick to erect and economical in cost, but provide good resistance to service demands. In addition to serving as the gravity-load-carrying system, floor diaphragms play an important role in the lateral-load-resisting system by transferring inertial forces between the diaphragm and shear walls.

Current design practice for precast structures makes use of the equivalent lateral force approach to determine seismic design loads[1]. Diaphragm design load at each level, F_{px}, is specified by a distribution from the equivalent lateral forces, F_i. This lateral load is applied along the diaphragm length according to the elastic horizontal deep beam model (or plate girder analogy)[2]. Diaphragm flexure is resisted by chord steel located at the extremities of the diaphragm. These chord forces are transferred to the lateral force resisting system to provide integrity of the diaphragm. The shear forces generated by the dynamic loading are resisted by the

[1] Assistant Professor, Lehigh University, Bethlehem, PA, Email: cjn3@lehigh.edu
[2] Doctoral Researcher, Lehigh University, Bethlehem, PA, Email: lic6@lehigh.edu

discrete connectors located between the diaphragm panels. These panel-to-panel connections along the joint are designed to transfer in-plane diaphragm shear forces, which vary due to shear force distribution in the deep beam model (Figure 0).

Although the beam model introduces a simple load path which is easily adapted to strength based design, the deformation capacity is ignored. To determine the force distribution to the lateral system and to calculate the structural drift, the floor system is assumed to be rigid. Thus the gravity load system is assumed to have the same displacement as the shear wall. Recent research[3,4,5], however, indicates that precast diaphragms may be subjected to large deformations under seismic loads. Under these conditions the gravity load system would undergo drifts several times that originally assumed. It is in question whether the gravity load system can safely meet the deformation demand.

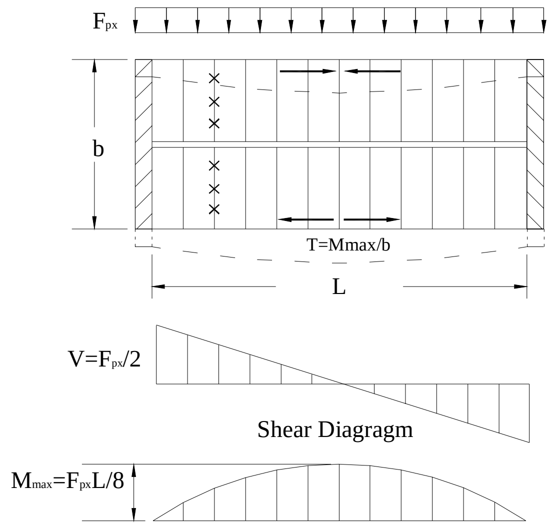

Figure 0: Diaphragm beam analogy

Compatibility of the joint connectors under elevated demands is a concern for diaphragm systems. The design philosophy assumes that all the connections equally resist the shear force. Under elevated demands the compression region of the diaphragm may resist higher shear forces than the tension side. In addition the shear ductility may be inadequate to sustain large deformations. This may result in a progressive failure of the diaphragm connectors along a joint. Furthermore, it is doubtful that shear strength is the only controlling factor which affects diaphragm joint behavior. Observed diaphragm failures from recent earthquakes[6,7] and seismic analysis[3,4] demonstrates that the actual diaphragm performance may not match current design assumptions due to, complicated load paths, inelastic behavior that cannot be prevented under large earthquake demands, and asymmetric and higher-mode diaphragm response.

Precast diaphragm behavior is dependent on a complex interaction of force combinations, diaphragm deformations, and load history. To comprehensively evaluate the performance of diaphragms under seismic demands, methods for determining diaphragm deformation are critical. Making the gross assumption that the precast element is rigid relative to the connectors, evaluating the diaphragm response begins with proper understanding of the connector response.

DOUBLE-TEE CONNECTION DATABASE

Connection details of double-tee panels vary in accordance with design requirements and precast manufacturing preference: In high seismic zone, such as California, engineers have relied on a cast-in-place topping slab overlaying the panels to ensure structural continuity. A mechanical connector, embedded in precast panels during fabrication, is an alternative method used to join adjacent tee flanges in low or moderate seismic zone. This flange-to-flange connector is typically welded to the adjacent connector by a round/rectangular slug (bar/plate) between two exposed steel faces of embedded connectors. A combination of both the mechanical connectors and cast-in-place topping is commonly preferred to provide redundancy in seismic design. Construction requirements such as leveling of the tees often require the use of the welded connector even in low or moderate seismic regions.

Due to the wide variety of mechanical connector types in use, a thorough survey of connection details was conducted with US precast concrete producers and concrete hardware suppliers. Based on current knowledge the existing connection types are categorized in Table 1. Summary of industry feedback from 19 companies (Table 2) indicates that bent rebar connectors (DT3-1), straight rebar welded to plates (DT3-3) and proprietary connectors (DT3-5) are the most popular connectors in use.

Bent rebar connector (DT3-1) provides the lowest cost connector due to its ease of fabrication and low material cost. Due to its shallow profile it is able to fit in thin flanges and thus is used commonly in topped systems (i.e., 2” flange). Straight rebar with welded plate connector (DT3-3) is used as both web and chord connectors, but work for diaphragm-to-wall collectors as well. Recent tests[8,9,10] indicate that manufactured connectors (DT3-5) are relatively ductile and easily installed in precast panels.

<table>
<tr><th colspan="5">Table 1: DT connection details database</th></tr>
<tr><td colspan="2">DT1
Topping with WWR</td><td colspan="3">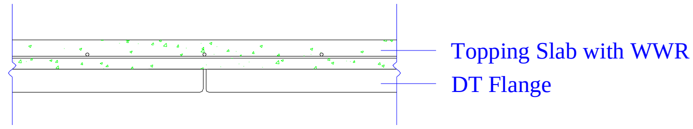
</td></tr>
<tr><td colspan="2">DT2
Topping & mechanical connectors</td><td colspan="3">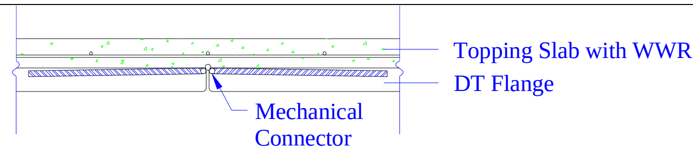
</td></tr>
<tr><td rowspan="5">DT3
Mechanical connectors</td><td>DT3-1
Embedded bent rebar only</td><td>DT3-1A: with recess
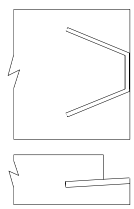</td><td>DT3-1B: no recess
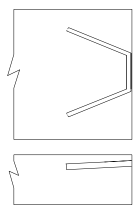</td><td>DT3-1C: Rebar w/ additional vertical bent
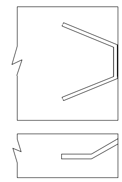</td></tr>
<tr><td>DT3-2
Embedded bent rebar welded to steel plate(angle)</td><td>DT3-2A: Bent rebar & angle
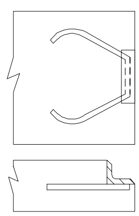</td><td>DT3-2B: Continuous bent bar & plate
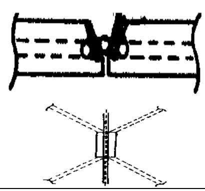</td><td>DT3-2C: Bent bar & plate
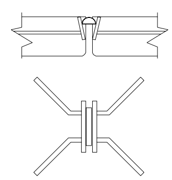</td></tr>
<tr><td>DT3-3
Embedded straight rebar welded to embedded steel plate</td><td>DT3-3A: rebar welded 90 degree to plate
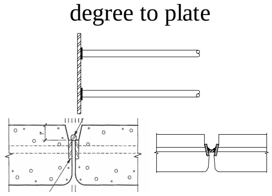</td><td>DT3-3B: Nelson Stud
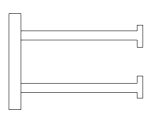</td><td>DT3-3C: rebar welded 45 degree to plate
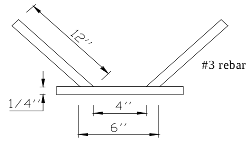
</td></tr>
<tr><td rowspan="2">DT3-4
Cover plate</td><td>DT3-4A: embedded steel plate & straight rebar
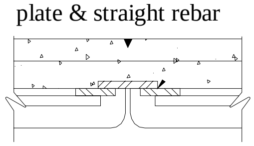</td><td>DT3-4B: embedded angle & straight rebar welded to vertical leg
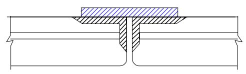</td><td>DT3-4C: : embedded angle & straight rebar welded to horizontal leg
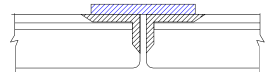</td></tr>
<tr><td>DT3-4D: embedded steel plate & bent rebar
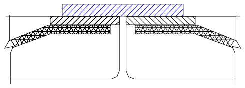</td><td>DT3-4E: Flexible angle cover plate[11]
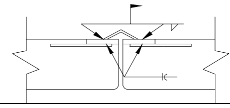</td><td>DT3-4F Cover plate with stud & rebar anchorage
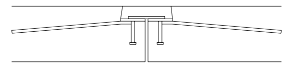</td></tr>
</table>

Table 1: DT connection details database

	DT3-5 Manufactured connector	DT3-5A: JVI connector[8,9] 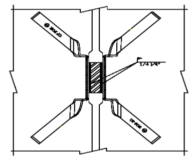	DT3-5B: Dayton connector P11[10] 	DT3-5C: Dayton P11B connector[10]: 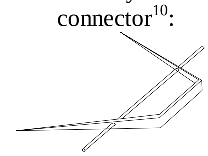
		DT3-5D: Dayton Channel connector[10]: 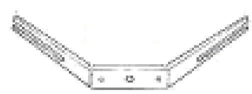	DT3-5E: Dayton Waffle connector[10]: 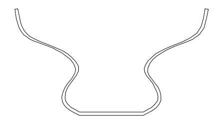	DT3-5F: Precast Engineering connector[12] 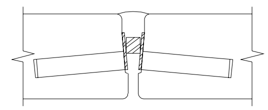
	DT3-6 Special details	DT3-6A: Exposed rebar[13] 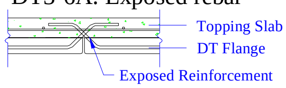	DT3-6B: Angle welded to WWR [14] 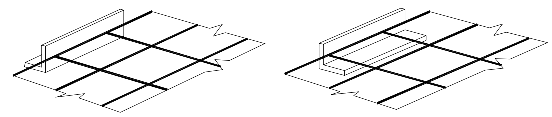	

Table 2: Summary of industry feedback

Connector ID	A	B	C	D	E	F	G	H	I	J	K	L	M	N	O	P	Q	R	S	Total
DT1						■			■											2
DT2		■				■	■				■									4
DT3-1		■	■				■		■				■	■			■		■	8
DT3-2			■								■									2
DT3-3		■	■			■		■	■							■		■	■	8
DT3-4			■					■	■			■		■	■					6
DT3-5	■	■		■		■	■	■	■		■		■		■		■	■		12
DT3-6					■					■										2

Double-Tee Connection Performance Database

To study the behavior of diaphragm systems under earthquake loading the performance of individual connectors must be known. The pilot experiments on shear connector traces back to 1968 when Venuti[15] conducted 68 monotonic shear tests on two bent rebar connection types DT3-1A and DT3-2B. Since then many studies have been conducted to qualify the performance of flange-flange shear connectors.[8-11, 14-18] Connections were evaluated under horizontal shear loading, horizontal tension loading, vertical shear loading, and horizontal shear loading with constant tension. Studies were conducted both monotonically and cyclically.

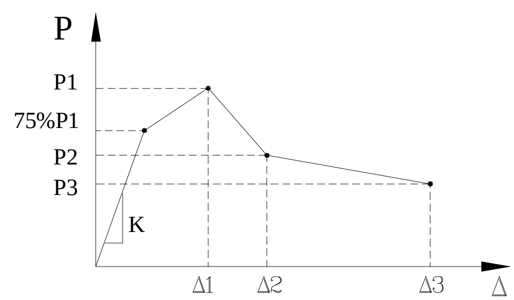

Figure 0: Database model basis

As a first step in evaluating the diaphragm performance a comprehensive database of load-deformation responses were collected, Table 3. All data is summarized from previous testing reports[8-11,14-18] in chronological order. Data is compared with regard to a pair of connectors. This includes two connectors on both sides of the slab gap. For the single connector test results, the original deformation value has been doubled and the stiffness is reduced by half to represent the connector pair behavior; these results are highlighted in red. Initial stiffness is measured at the point where load reaches 75% peak load value. All the measured force-displacement responses show that after peak load is reached, the connector strength quickly drops down to the residual value. Connector eventually reaches its displacement limit. To represent these points three load-deformation points (P_i, Δ_i) are tabulated as shown in Figure 0.

Database Discussion

As mentioned, a variety of connection types are in use. PCI design handbook[2] provides guidance on the strength capacity of the DT3-1 and DT3-3C connections. Precast diaphragm design is done purely on a force based approach with no guidance on the estimation of displacement. To evaluate this issue the force-displacement responses of Table 3 can be used. Caution, however, should be placed on the application of the database. Due to the importance of connection strength in the last 30 years most tests were aimed at determining force capacity. The majority of tests only consider the shear response, a small portion include tension and compression behavior, and a smaller number examine the combined shear and tension response. In spite of these limitations, the database provides a first step tool for examining the deformation characteristics of connectors.

Table 3: DT/DT web connector performance database

Ref.	Connector ID	Test [a]	Initial stiffness K (kips/in)	P1 (kips)	Δ1 (in)	P2 (kips)	Δ2 (in)	P3 (kips)	Δ3 (in)	Failure mode[b]
W. Venuti (1968) [15]	DT3-1A(M) [c]	MV	110	15	0.14	13	0.2	12	0.35	3
	DT3-1A (N)	MV	180	22	0.14	15	0.25	12	0.35	
	DT2 (KK) (with DT3-1A)	MV	400	53	0.11	40	0.2	25	0.35	
	DT2 (LL) (with DT3-1A)	MV	335	60	0.15	55	0.2	36	0.35	
	DT2 (KK) (DT3-2B)	MV	295	60	0.17	abrupt failure at P1				
	DT2 (LL) (DT3-2B)	MV	305	55	0.23	43	0.35	33	0.5	
CTC. (1974) [11]	DT3-4B	MV	490	20	0.06	–force control–			N/A	1 & 2
	DT3-4C	MV	1250	20	0.03	–force control–			N/A	
Aswad (1977) [16]	DT3-1B	MV&CV	400	10	>0.06	N/A	N/A	N/A	N/A	3
		MVT	60	10	0.8	N/A	N/A	N/A	N/A	N/A
	DT3-4A	MV	240	20	0.2	14	0.6	13	0.96	2
		MT	N/A	5	N/A	2	N/A	N/A	N/A	N/A
R. Spencer (1986) [17]	DT3-2A (MS bar)	(MV&)CV	345	43	0.2	N/A	N/A	18	1	4
	DT3-1A	(MV&)CV	915	40	0.1	N/A	N/A	26		2,4,5,6
	DT3-1B	(MV&)CV	300	33	0.17	N/A	N/A	28		2,3
	DT3-1C	(MV&)CV	285	25	0.12	15	0.25	12		2,3,5,6
	DT3-1C (w/ 90deg. Bend)	(MV&)CV	345	26	0.2	N/A	N/A	10	1	3,4,5
Kallros (1987) [14]	DT3-1B	CV	820	17	0.05	14	0.05	-	-	2
	DT3-4C	MV;CV	320	15	0.06	10	0.65	-	-	3
	DT3-1A (2" slab)	MV;CV	270	20	0.11	13	0.35	10	0.55	3,8
	DT3-1A (3" slab)	MV;CV	690	20	0.16	16.8	0.31	16	1	2,3,8
	DT3-6B (a)	CV	245	15	0.07	8	0.3	8	1	2
	DT3-6B (b)	CV	220	15	0.14	11	0.25	-	-	2
Pincheira (1998) [18]	DT3-3C	MV	450	16	0.05	15	0.15	2	0.2	2,4
		CV	360	17	N/A	N/A	N/A	N/A	N/A	2
		MT	210	15	0.32	2	0.36	-	-	2

Table 3: DT/DT web connector performance database

Ref.	Connector ID	Test [a]	Initial stiffness K (kips/in)	P1 (kips)	Δ1 (in)	P2 (kips)	Δ2 (in)	P3 (kips)	Δ3 (in)	Failure mode [b]
		CT	265	13(T) -31(C)	N/A	N/A	N/A	N/A	N/A	2,4
		MVT-V	300	9	0.05	8	0.12	1	0.18	2
		MVT-T	330	9	0.1	8	0.16	1	0.19	
		CVT-V	320(@ T) 870(@C)	8(@ T) 30(@ C)	N/A	N/A	N/A	N/A	N/A	2
		CVT-T c	535(@T)	8(@T) 30(@ C)	N/A	N/A	N/A	N/A	N/A	
JVI (2000) [8]	DT3-5A (plain steel B)	MV	580	20	0.06	15	0.24	13	1.5	4,8
		CV	565	20	0.07	11	0.18	10	0.6	2
		MT	235	10	0.81	10	1.72	6	2.7	10
		MvV	80	7	0.19	brittle failure at ultimate load				3
		MVT	265	18	1.24	10	1.74	5	2.34	8
		CVT	195	15	0.12	9	0.92	-	-	2
Dayton (2002) [10]	DT3-5B	MV	100	8	0.16	7	0.78	-	-	8,9
		MT	45	3	0.25	3	0.65	-	-	3,8
	DT3-3B	MV	150	30	0.29	10	0.43	8	0.52	4,7
		MT	480	15	0.11	0	0.78	-	-	5
	DT3-5D	MV	85	20	0.45	10.8	0.6	brittle failure		10
		MT	110	9	0.47	8	0.86	7	1.05	10
		MVT	420	20	0.14	3	0.55	-	-	2,3
		CVT	75	17	0.25	3	0.65	-	-	2,3
		CV	80	17	0.28	3	0.48	-	-	2,3
	DT3-5E	MV	250	12	0.1	12	0.27	12	0.5	10
		MT	40	6	0.65	4	1	-	-	10
	DT3-5C DT3-5C	MV	130	10	0.17	8	0.18	6	0.63	8,9
		MT	65	5	0.24	2	0.35	2	0.6	8
		MVT	155	7	0.1	4	0.5	4	1	2,3
		CVT	85	7	0.14	3	1	-	-	2,3
		CV	100	9	0.12	5	0.3	5	1	2,3

a. M-Monotonic, C-cyclic, T-tension, V-shear, v-vertical shear, VT-combined shear and tension
b. Failure mode: 1-cover plate or bar twisting; 2-bar fracture; 3-concrete spalling or crushing in compression; 4-weld fracture; 5-concrete splitting; 6-Bond slip; 7-concrete breakout; 8-leg pullout; 9-leg buckling; 10-faceplate rupture (bent plate connector)
c. DT3-1A(M): No.4 bar , 2.5" thick flange; DT3-1A(N): No.5 bar,2.5" thick flange
DT2(KK): No.4 bar, 2" thick flange&2"topping; DT2 (LL): No.4 bar, 2.5" thick flange&2"topping

Flange Connector Failure Mechanisms

Four types of failure mechanisms are common in these connector tests: 1) fracture of an anchorage leg; 2) buckling of an anchorage leg; 3) pullout of an anchorage leg; and 4) concrete spalling or crushing above or below the anchor leg. Additional, though less common, failure modes include twisting, weld failure, concrete slab splitting, and breakout. Premature brittle failure severely affects the connection strength and ductility. Therefore, to achieve a reliable capacity a ductile connector failure mechanism must be identified and implemented through capacity design. Based on the observed failure modes discussed, it is recommended that a tensile anchorage leg yield mechanism be used.

CONNECTOR DESIGN STRENGTH

Although a variety of connection types result from different connection configurations, the connections can be divided into two basic groups due to current design models, bent bar group and embedded steel plate group:

Bent Bar Shear Connection

Bent rebar connector (also called ‘hairpin’ connector) are fabricated by bending the rebar at an angle from 30 to 90 degrees with 45 degrees being the most common. The pair of connectors embedded in two adjacent precast panels are connected by welding a rebar slug between them (Figure 0). The shear capacity of the mechanical hairpin connector is typically analyzed by the truss analogy. The nominal shear resistance of a connector is equal to the component of the yield forces in the bars[2].

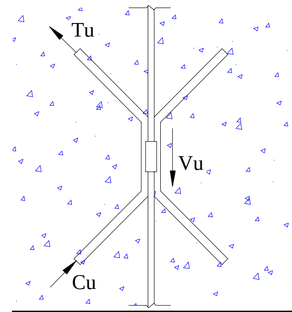

Figure 0: Truss model

$$C_n = T_n = A_s f_y \text{ (Eq.1)} \quad V_n = (C_n + T_n)\cos\theta = \sqrt{2} f_y A_s \text{ for } \theta = 45^\circ \text{ (Eq.2)}$$

Embedded Steel Plate Shear Connection

The second generic connection is composed of a steel plate welded to a reinforcing bar embedded in the panel (DT3-3, DT3-4). The calculation of shear strength was modified by Spencer considering the concrete bearing contribution at the end of the embedded steel plate[17]. It was suggested that the concrete bearing force F_P should be added to the tension bar resistance if bearing strength is greater than the resistance from the compression leg, C_n. This formulation directly accounts for the enhancement due to the concrete bearing contribution.

$$V_n = F_p + \frac{\sqrt{2}}{2} f_y A_s \text{ when } F_p \geq Tc_n \text{ (Eq.3)} \qquad \& \qquad V_n = \sqrt{2} f_y A_s \text{ when } F_p < C_n \text{ (Eq.4)}$$

$$\text{Where, } F_p = f_c' A_p \text{ (Eq.5)}$$

Erection of double tee precast panels requires that the panel to panel connector be welded in the field. The welding process produces a heat expansion of the plate which can result in break out of the concrete around the steel plate. Thus, typical construction practice requires that a space be included to allow for heat expansion from welding. From a design strength view this eliminates the occurrence of a plate bearing mechanism. Furthermore, in comparison with experimental results the design strength using the truss model is not always conservative Table 4.

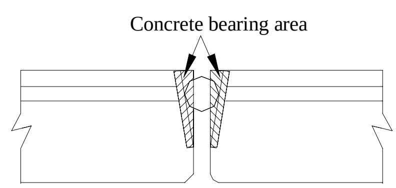

Figure 0: Concrete bearing area, A_p

To provide a comprehensive estimate, a two part shear estimation is recommended. The model evaluates the tension, V_t, and compression response, V_c separately. The tension contribution is equal to the yield strength of the tension leg. The compression response is based on the bearing strength of the compression leg. Previous research[16] observed that the crack propagates along the compression leg near the peak load. At this level a $12d_b$ bar length was activated in bearing on the concrete. In accordance with this observed performance, a conceptual modification to shear strength that includes the effective concrete bearing strength along the compression leg as shown. Modified peak strength is:

$$V_n = V_t + V_c \text{ (Eq.6)}$$

$$V_t = \frac{\sqrt{2}}{2} A_s f_y \text{ (Eq.7)} \qquad V_{cb} = \frac{\sqrt{2}}{2} A_s f_y \text{ (Eq.8)} \qquad V_{cc} = 12 f_c' \cdot d_b^2 \cos\theta \text{ (Eq.9)}$$

$V_c = V_{cb}$ when $V_{cb} > V_{cc}$ & $V_c = V_{cb}$ when $V_{cb} > V_{cc}$

Where d_b is leg bar diameter, θ is angle of the bent rebar, f_y is the yield strength of the rebar, and f'_c is the concrete compressive strength.

The modified design strength in Table 4 provides an accurate estimation of the capacity. This modification provides the designer with a tool to define the type of failure mechanism desired. For example the rebar can be sized to preclude bearing failure of the compression leg thus ensuring a ductile mechanism. In addition the improved estimate of strength allow for a safer capacity design of the brittle components such as the weld.

The limitation of this method is that the reinforcement leg must be properly developed into the double-tee flange to avoid premature pullout. In addition to avoid embrittlement due to welding, it has been recommended that the welded slug should be at least $2d_b$ from the cold bend[2]. To ensure that this failure does not occur, it is further recommended that the $2d_b$ distance be taken from the end of the bend and not the center of the bend.

Shear Connector Residual Strength

All connectors undergo a decrease to half their load-carrying capacity by the time their deformation limit is reached (Table 4). This behavior is due to the local concrete failure mechanism that occurs as the compression bar bears on the concrete as it starts to buckle[8,9,11,12,13]. The compression leg loses its contribution to the shear resistance except that the tension leg continues to carry the load. Therefore, strength at failure is reduced down to the resistance of the tension leg, which can be taken as approximately half of the peak value, *P1*.

Table 4: Comparison of failure load with peak load

Ref.	Connection	P1 exper. [kips]	PCI V_n [kips]	Modified V_{n-M} [kips]	$\frac{V_n}{P_1}$	$\frac{V_{n-M}}{P_1}$	Vt [kips]	P3 [kips]	P3/P1
Venuti	DT3-1A(M)	15	11	16	0.67	1.1	6	12	0.80
	DT3-1A(N)	22	18	25	0.73	1.1	9	12	0.55
Spencer	DT3-1A	40	38	38	0.95	0.95	20	26	0.65
	DT3-1C	25	25	28	1	1.1	13	12	0.48

Configuration Effects and Recommendations

Using the database of research results the effect of variations in connector bar size, panel thickness, connector configuration and other parameters can be studied. It is concluded that:

1) Rebar size and yield strength are the most important factors in determining connector strength. Brittle failure is likely to occur in connections fabricated from high yield strength bars, and connections with lower yield stress are able to sustain more loading cycles at lower load levels after the maximum strengths have been reached.[14,17] Low yield bars become plastic prior to crushing thus can sustain large deformation without significant panel damage. In contrast, high yield strength bars sustain local concrete crushing before reaching yield. Consequently, connections with relatively low yield strengths are desirable.

2) Connection behavior is influenced by the panel thickness.[14,15,17] Minor increase of panel thickness (2” to 2.5” panels) does not have a serious effect on the connection strength.[15] However, a decrease of a 1.0” thickness greatly reduces the connection strength. Connection stiffness and deformation capacity is significantly enhanced due to less concrete spalling and crushing.

3) The angle of bend does not remarkably change connection performance[15], but does affect the connection load path. Moderate angle require that the connection carry the shear load by tension and compression bar resistance, while large angles (i.e., 90 degree) changes the mechanism to one of shear friction and concrete bearing. Therefore, an unpredictable brittle failure is likely when large bar angles are used. Small bend angle is also not recommended due to the tendency toward a pullout failure. A 45 degree bend is recommended if space is available. For tight locations a 60 degree bend should be used.

4) A recess near the connection is desirable for pretopped panels to improve the connection capacity[17]. The recess allows for the connector to be located near the mid-depth of panel. This increases the cover of the bar which decreases the susceptibility to local concrete breakout.

Effect of Topping on Shear Resistance

To allow for volume change and shrinkage deformations, topping slabs are commonly tooled or pre-cracked along each panel-panel flange joint. In some instances the joint may be uncracked, for these conditions the strength contribution can be significant. Test on topped connections were conducted by Venuti.[15] Test data illustrates that effect from the topping slab on shear capacity is substantial. Table 5 compares the untopped and topped connection shear strength for DT3 connectors. Addition of topping can increase the strength capacity by greater than 3. By comparison, the topping does not greatly affect maximum deformation capacity (Table 3). A topped connection also exhibits a considerable increase in stiffness. Typically the stiffness can be more than doubled (Table 5).

Table 5: Shear strength comparison on topped and untopped connections

	DT3-1A #4 Untopped	DT3-1A #4 2" Topping	DT3-1A #5 Untopped	DT3-1A #5 2" Topping
PCI design strength (kips)	10	-	16	-
Measured shear strength (kips)	15	53	22	60
Measured shear strength due to connector (kips)	15	15	22	22
Actual shear strength due to 2" topping (kips)	-	53-15=38	-	60-22=38
Concrete shear strength in the topping $V_c = A_{cv}(2\sqrt{f_c'})$	-	13	-	13
Initial stiffness (kip/in)	110	400	180	335

The WWR plays a significant role in providing the increase in the shear strength and stiffness for topped diaphragms. As shown in Table 5 the concrete provides a third of the measured topping shear strength. The shear design strength of topped connections can be obtained by superposing the shear strength of the topping with that of the shear connector (Eq.10). ACI[20] recommends a relation for shear capacity of the topping assuming a shear friction model. This topping shear contribution, $V_{topping}$ can be computed from Eq. 11 where A_{cv} is the gross area of concrete cross section ρ_n is the reinforcement ratio perpendicular to the joint.

$$V_n' = V_{connector} + V_{topping} \text{ (Eq.10)} \qquad V_{topping} = A_{cv}\rho_n f_y \text{ (Eq.11)}$$

Shear Compliance with Tension Deformation

Under earthquake demands, the panel-to-panel connections are subject to complicated loads of combined shear and tension forces or shear with large tensile deformation at critical areas. Database comparison was conducted to identify the sensitivity of shear response to the presence of tension. Three different methods were used in prior research: (1) shear with constant tension force, (2) shear with constant tension deformation, and (3) shear with proportionally increasing tension force. For the hairpin connector DT3-1, applying a constant tension force decreases the shear stiffness and strength, and provides an increase in deformation capacity[15,16]. The use of a constant tension force improves the flexibility of the connection by imparting a continuous pullout on the reinforcement. This changes the failure mode from a brittle concrete fracture mode to a ductile reinforcement yield mechanism. Under a constant opening, previous research[8,9] has resulted in a reduction in stiffness by a factor of 2. Providing a proportionally increasing tension force however decreases the shear strength by up to 50% but does not greatly affect the deformation and initial stiffness[18].

ANALYTICAL MODELING OF PRECAST DIAPHRAGMS

FEM Methods

A simple elastic deformation, nonlinear pushover, or nonlinear time-history response can be conducted with the connector performance database (Table 3). This information can be used to establish rigidity of the

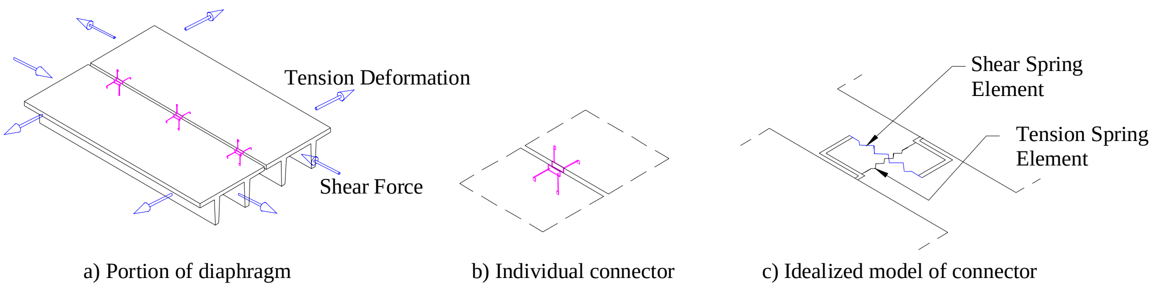

Figure 1: Connector modeling

An example model is built and analyzed using DIANA Finite Element Analysis 8.1[27]. The double tee panels are modeled as four-node quadrilateral isoparametric flat shell elements which are a combination of plane stress and plate bending elements. The concrete elements are modeled as elastic for simplicity. Nonlinearities are included in the connectors which are modeled as discrete interface elements. Nonlinearity of the connectors can be modeled using any of the simplified multi-linear shear and tension load – deformation relationships previously defined. For this example the shear and tension response measured by Pincheira and Oliva (1998)[18] was used (Table 3). Compression is modeled with a rigid spring.

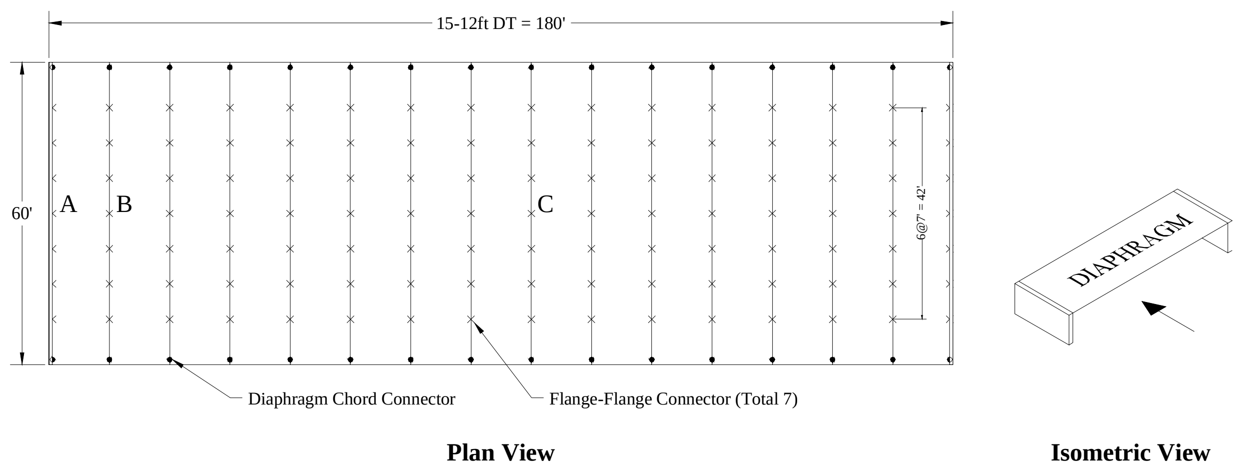

Figure 2: Simple diaphragm model

A 60-ft x 180-ft diaphragm constructed of 12-ft wide double tees is evaluated in this example. Vertical restraints are placed at the ends of the double-tees at the bottom of their webs. Vertical restraint is also provided at each panel-panel and panel-wall connector. The tension chord consists of 2-#6 bars. The discrete connector spring assumes that the bars achieve an unbonded length of $40d_b$; no shear resistance is provided. The spring properties used for the components are illustrated in Figure 3. The system is evaluated for the design lateral load and an earthquake time history recorded during the Northridge earthquake Figure 4.

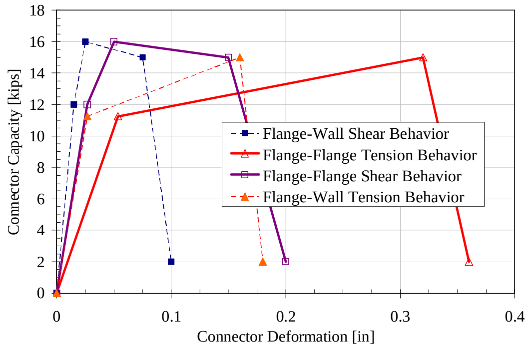

Figure 3:Diaphragm spring models

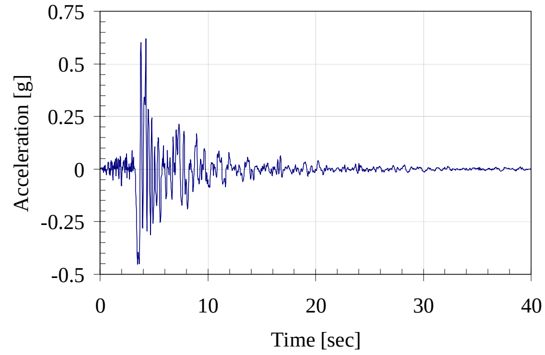

Figure 4: Northridge earthquake ground motion

At low demands the connectors respond close to a first mode response (Figure 5). The stress distribution in the panels (X-Dir) indicates that the web connectors are active in resisting the flexural demands. This contribution should be considered when evaluating the diaphragm deformation. The shear forces are transferred to the panels primarily in the compression and tension chord regions of the diaphragm (see Figure 5 b & d). The out-of-plane stiffness of the supporting walls affects the stress distribution in the diaphragm. Due to this restraint the connectors can be subjected to elevated stresses at the interface. Improper attention to these conditions can result in an underestimation of demand.

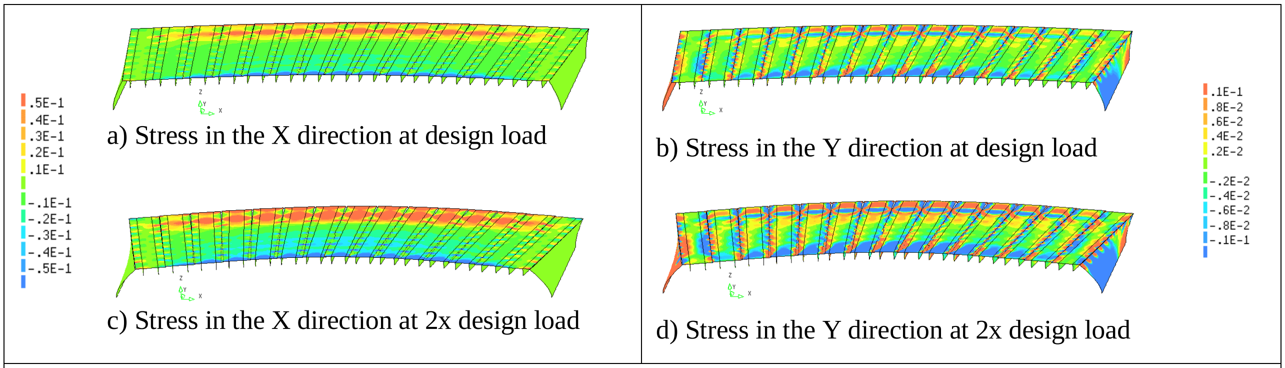

Figure 5: Stress distribution under design load

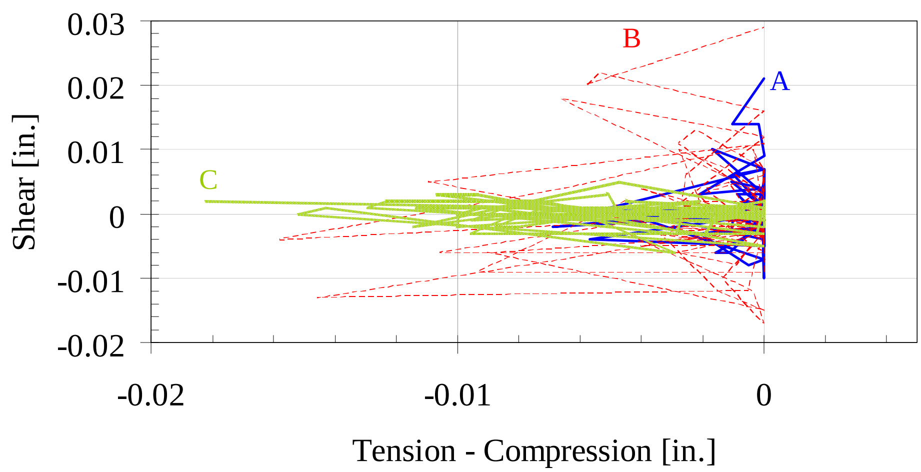

Figure 6: Connector deformations

The deformation response is plotted for three connectors along their shear and tension axes (Figure 6). The deformation history is highly dependent on the location within the diaphragm. Connectors located at the center of the diaphragm are subjected to less shear and higher flexural effects (C) while connectors at the boundaries (A & B) are subject to greater shear effects. In all cases the diaphragm connections are subjected to a combination of demands in both shear and tension.

Simplified Analytical Methods

To compare with FEM results a simplified is used to compute deformation from the deep beam model. The model assumes that the diaphragm deformations occur only at the joints and that the panels remain comparatively rigid under seismic loads. The diaphragm deformation is composed of two parts: shear deformation and flexural deformation. The shear deformation is resisted by the shear connectors along the joint. Due to the small size of the chord reinforcement the shear contribution of the chord is ignored in this model. Joint shear deformation can be determined by dividing the joint shear force by the total and joint stiffness. The total joint stiffness can be computed by summing the stiffness of all the connectors along the joint. Using this method, the diaphragm deformation due to shear can be computed for the previous model. Figure 7 presents the shear deformation contribution from the panel to panel connectors (V w/ web). The flexural diaphragm deformation can be computed from the joint rotational stiffness and applied moment. Assuming that the joint opens relative to the bottom fiber, the tension contribution of each web and chord connector can be determined. An effective rotational stiffness, K_r, can be computed by $K_r = \sum K_t \cdot d_i^{\,2}$, where K_t is the connector tension stiffness and d_i is the distance to the connector from the bottom fiber. The corresponding estimated story drift is presented as M&V w/ Web in Figure 7. In contrast, the diaphragm deformation ignoring the web connector tension stiffness (M&V w/o web line) is twice as large. The shear connectors clearly play a significant role in resisting the flexural deformations of the diaphragm. Joint shear deformation contributes to approximately a third of the diaphragm deformation.

Due to the stiffness of the supporting shear walls the ratio of diaphragm to shear wall deformation is far greater than the IBC[26] rigid diaphragm drift limit of 2.0. Consequently the diaphragm studied should be considered as a flexible diaphragm. UBC[1], however, specifies that the diaphragm can be considered rigid if the aspect ratio is no more than 3:1. This discrepancy should be examined further with experimental and analytical validation.

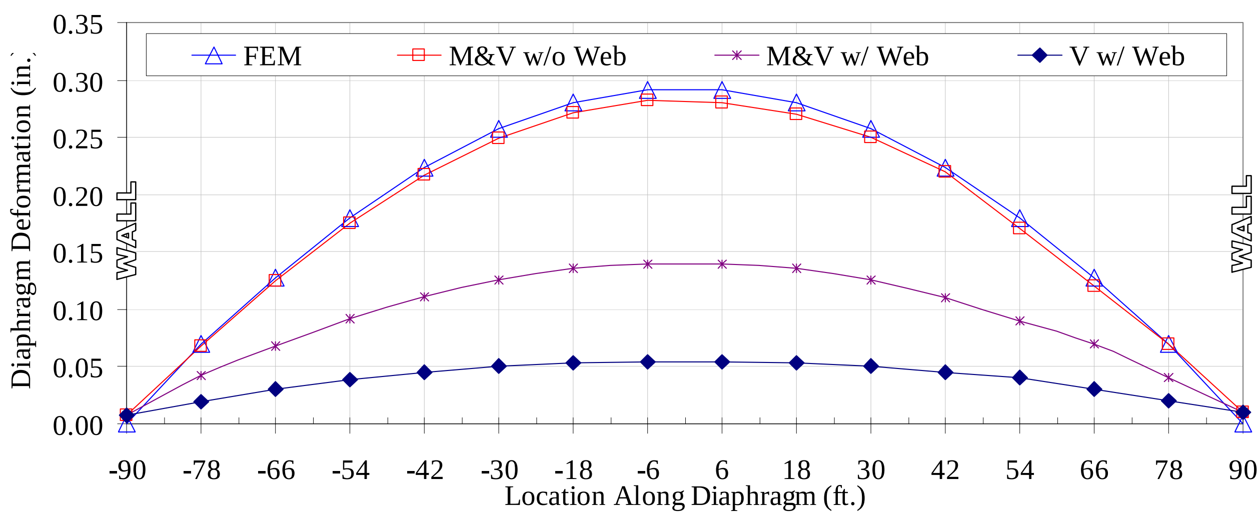

Figure 7: Diaphragm deformation

CONCLUSION

From the research presented, the following conclusion can be made:

- Diaphragm panel-panel connections can be classified into three general categories. Discrete connectors, topping with WWR and topping with discrete connectors.

- Discrete connectors can be further classified into six additional subcategories based on their configurations.

- Based on industry feedback, three configurations are commonly used: Bent rebar, straight rebar welded to a face plate, and manufactured connectors.

- The performance of connectors is tabulated from all available research results. This provides a powerful research database that can be used for prediction of diaphragm deformations.

- To support inelastic diaphragm displacements under earthquake motions a ductile connection failure mechanism is preferred. This can be achieved by capacity design of a yield mechanism in the connector.

- An analytical method is proposed to predict the actual capacity of the connector. This response is based on bearing failure of the compression leg and tensile yielding of the tension leg. The formulation provides an accurate estimate of strength.

- From the limited testing results topping slabs with WWR provide significant contribution to the joint shear resistance.

- The majority of previous connection tests were conducted under pure shear or pure tension to examine the strength of the connector. The limited research conducted on the behavior of connections under combined loading indicates that there exists a strong coupling between shear strength and tension deformation. Further investigations are strongly recommended.

- FEM methods can be successfully used to examine the nonlinear response of diaphragms under earthquake motions. The results correlate with simplified hand calculations.

- A simplified method for computing diaphragm deformations is proposed. This method can be used by designers to approximate diaphragm deformations.

- Preliminary estimates of diaphragm deformations by the methods presented indicate that they may be much larger than currently assumed.

ACKNOWLEDGEMENTS

The research was supported by a grant from the Precast Prestressed Concrete Institute and the Pennsylvania Department of Transportation and a grant from the Commonwealth of Pennsylvania, department of Community and Economic Development, through the Pennsylvania Infrastructure Technology Alliance (PITA).

REFERENCES

1. ICBO, Uniform Building Code, 1997 Edition, International Conference of Building Officials, Whittier, CA, 1997

2. PCI Design Handbook, Precast and Prestressed Concrete, Fifth Edition, Chicago, IL, 1999

3. Fleischman, R.B., Sause, R., Pessiki, S., and Rhodes, A.B., “Seismic Behavior of Precast Parking Structure Diaphragms,” PCI Journal, January-February 1998, V. 43, No.1, pp.38-53

4. Fleischman, R.B., Farrow, K.T. Eastman, K., "Seismic response of perimeter lateral-system structures with highly flexible diaphragms", Earthquake Spectra., May 2002, V.18, No.2, pp.251-286
5. Nakaki, S.D., "Design Guidelines for Precast and Cast-in-place Concrete Diaphragms" Technical Report, EERI Professional Fellowship, Earthquake engineering Research Institute, April, 2000
6. Wood, S.L., Stanton,J. F., Hawkins, N. M., "New Seismic Design Provisions for Diaphragms in Precast Concrete Parking Structures", PCI Journal, January-February 2000, V.45, No.1, pp.50-65
7. Iverson, J.K., Hawkins, N.M., "Performance of Precast/Prestressed Concrete Building Structures During Northridge Earthquake", PCI Journal, March-April 1994, V.39, No.2, pp.38-55
8. Oliva, M.G., "Testing of the JVI Flange Connector for Precast Concrete Double-tee Systems", Structures and Materials Test Laboratory, University of Wisconsin, June 2000
9. Shaikh, A.F., and Feile, E.P., " Testing of JVI Vector Connector", Structural Engineering Laboratory, September 2002
10. Dayton/Richmond Concrete Accessories, "Dayton/Richmond Flange-to-Flange Connector Tests", Miamisburg, Ohio, March, 2002
11. Concrete Technology Corporation, "Tests of Shear Connectors Report", CTA-74-B8/9, pp.55-62
12. Precast Engineering, Connection details feedback sheet, May 2003
13. Applied Technology Corporation, Connection details feedback sheet, October 2003
14. Kallros, M.K., " An Experimental Investigation of the Behavior of Connections in Thin Precast Concrete Panels Under Earthquake Loading", M.S. Thesis, Civil Engineering Department, University of British Columbia, British Columbia, Canada, April 1987
15. Venuti, W. J., "Diaphragm Shear Connectors between Flanges of Prestressed Concrete T-Beams", PCI Journal, Vol.15, No.1, February 1970, pp.67-78
16. Aswad, A., "Comprehensive Report on Precast and Prestressed Connections Testing Program", Research Report, Stanley Structures, Inc, Denver, Colorado, June-October 1977.
17. Spencer, R. A., and Neille, D.S., "Cyclic Tests of Welded Headed Stud Connections," PCI Journal, Vol.21, No.3, May-June 1976, pp.70-83
18. Pincheira, J. A., Oliva, M.G., and Kusumo-Rahardjo, F. I., "Tests on Double Flange Connectors Subjected to Monotonic and Cyclic Loading", PCI Journal, May-June 1998,V.43, No.3, pp.82-96
19. PCI, Design and Typical Details of Connections for Precast and Prestressed Concrete, Prestressed/Precast Concrete Institute, Chicago, 1988
20. ACI Committee 318, "Building Code Requirements for Structural Concrete," ACI 318-02, American Concrete Institute, Farmington Hills, MI, 2002
21. Cleland, N., "Diaphragm Design", Committee Report, PCI Seismic Committee, Prestressed /Precast Concrete Institute, October, 2001
22. Clough, D.P., "Considerations in the Design and Construction of Precast Concrete Diaphragms for Earthquake Loads," PCI Journal, March-April 1982, V.27, No.2, pp.78-93
23. Cleland, N., and Ghosh, S.K., "Untopped Precast Concrete Diaphragms in High-Seismic Applications," PCI Journal, November-December 2002, Vol.47, No.6, pp.94-99
24. Rhodes, A. B., "Seismic Performance of Precast Parking Structures: Transverse Direction", M.S Thesis, Civil Engineering, Lehigh University, Bethlehem, PA, September, 1995

25. Hawkins, N.M. and Ghosh, S.K., “Proposed Revisions to 1997 NEHRP Recommended Provisions for Seismic Regulations for Precast Concrete Structures Part 3-Diaphragms”, PCI Journal, November-December, 2002, V.45, No.6, pp.50-59

26. ICC, International Building Code, International Code Council, Country Club Hills, IL, 2003

27. Witte, F. C., et. al., *DIANA – Finite Element Analysis*. User’s Manual: Release 7. TNO Building Construction and Research. Delft, the Netherlands, 1998.